

## EFFECT OF DIFFERENTIALLY HEATING AND CONSEQUENT TRANSIENT BEHAVIOUR FOR NATURAL CONVECTION WITHIN AN ENCLOSURE OF SINUSOIDAL CORRUGATED SIDE WALLS

Muhammad Noman Hasan<sup>1</sup>, Suvash C. Saha<sup>2</sup> and Y. T. Gu<sup>2</sup>

<sup>1</sup>Department of Mechanical Engineering, BUET, Bangladesh.

<sup>2</sup>School of Engineering Systems, Queensland University of Technology, Australia

### ABSTRACT

Unsteady natural convection due to differentially heating of the sinusoidal corrugated side walls of a modified square enclosure has been numerically investigated. The fluid inside the enclosure is air, initially as quiescent. The flat top and bottom surfaces are considered as adiabatic. The numerical scheme is based on the finite element method adapted to triangular non-uniform mesh element by a non-linear parametric solution algorithm. The results are obtained for the Rayleigh number,  $Ra$  ranging from  $10^5$  to  $10^8$  for different corrugation amplitude and frequency with constant physical properties for the fluid medium considered. The streamlines, isotherms and average Nusselt numbers are presented to observe the effect of sudden heating and its consequent transient behavior on fluid flow and heat transfer characteristics for the range of governing parameters. The present results show that the transient phenomena are greatly influenced by the variation of the aforementioned parameters.

**Keywords:** Transient Natural Convection, Sinusoidal Corrugation, Differentially Heating.

### 1. INTRODUCTION

Natural convection heat transfer and fluid flow in enclosed space has received considerable attention because of its importance in several thermal engineering problems. Cavities with regular geometries like rectangular or triangular enclosures have studies in a great extent. Such boundaries are easier to model and the flow patterns and circulations are less complex than an enclosure having complex profile like having sinusoidal surface. Applications of such complex models are found in the design of electronic devices, solar thermal receivers, uncovered flat plate solar collectors having rows of vertical strips, designing solar collectors, electric machinery, cooling systems of micro-electronic devices, geothermal reservoirs, crystal growth etc. For an enclosure, if the vertical walls are in different heated state and the bottom and the top walls are adiabatic, the fluid flow occurs due to the presence of a horizontal temperature difference. The temperature gradient is horizontal whereas the gravitational force acts perpendicularly downward. The orientation of these two vectors decides the direction of the circulation in the cavity. Some relevant investigations on transient natural convection and boundary layer development have been carried out [1–6]. The purpose of the present study is to have a through analysis on the development of thermal

layer and heat transfer for transient natural convection within a modified square enclosure for ranges of Rayleigh number ( $Ra$ ), Corrugation Amplitude ( $CA$ ) and Corrugation Frequency ( $CF$ ) of sinusoidal side walls.

### 2. PROBLEM FORMULATION

In the present investigation, transient natural convection within a modified square enclosure, with sinusoidally corrugated side walls, has been considered. The side walls are assumed to be differentially heated and the flat top and bottom walls are considered as adiabatic. The thermal behavior has been studied for various Rayleigh number,  $Ra$ ; corrugation amplitude,  $CA$ ; corrugation frequency,  $CF$ . The fluid media that has been considered to flow within the enclosure is air with Prandtl number,  $Pr$  of 0.72. The schematic diagram of the investigate enclosure has been shown in the fig 1. The Rayleigh number,  $Ra$  range for the investigation has been taken from  $10^5$  to  $10^8$ . The corrugation amplitude,  $CA$  for the investigation has been taken 0.1, 0.3 and 0.5. The corrugation frequency,  $CF$  for the investigation has been taken 1, 3 and 5.

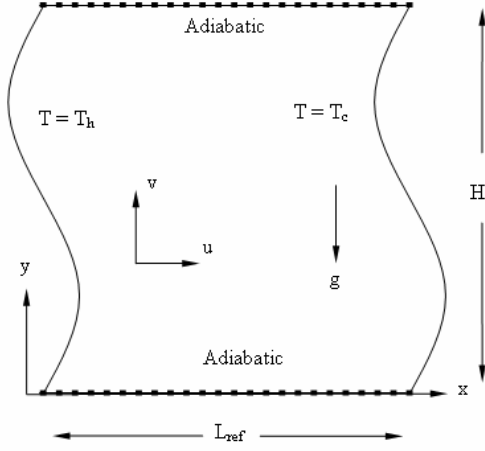


Fig 1. Schematic Diagram of the Physical Domain

### 3. MATHEMATICAL FORMULATION

#### 3.1 Governing Equation

A two-dimensional transient natural convective flow of an incompressible fluid within a modified square enclosure, with sinusoidally corrugated side walls, has been considered. Natural convection is governed by the differential equations expressing conservation of mass, momentum and energy. All the considered models are modified square enclosure, with sinusoidally corrugated side walls. These side walls are assumed to be differentially heated. The viscous dissipation term in the energy equation has been neglected. The Boussinesq approximation is invoked for the fluid properties to relate density changes to temperature change and to couple in this way the temperature field to the flow field. That is, the fluid properties are assumed to be constant except for the density which is considered to vary linearly with temperature according to the Boussinesq approximation. Then the governing equations for transient natural convection can be expressed as follows:

$$\frac{\partial U}{\partial X} + \frac{\partial V}{\partial Y} = 0 \quad (1)$$

$$\frac{\partial U}{\partial \tau} + U \frac{\partial U}{\partial X} + V \frac{\partial U}{\partial Y} = -\frac{\partial P}{\partial X} + \text{Pr} \left( \frac{\partial^2 U}{\partial X^2} + \frac{\partial^2 U}{\partial Y^2} \right) \quad (2)$$

$$\frac{\partial V}{\partial \tau} + U \frac{\partial V}{\partial X} + V \frac{\partial V}{\partial Y} = -\frac{\partial P}{\partial Y} + \text{Pr} \left( \frac{\partial^2 V}{\partial X^2} + \frac{\partial^2 V}{\partial Y^2} \right) + \text{RaPr}\theta \quad (3)$$

$$\frac{\partial \theta}{\partial \tau} + U \frac{\partial \theta}{\partial X} + V \frac{\partial \theta}{\partial Y} = \left( \frac{\partial^2 \theta}{\partial X^2} + \frac{\partial^2 \theta}{\partial Y^2} \right) \quad (4)$$

#### 3.2 Normalization

To obtain these above normalized equations (1), (2), (3) and (4) into non-dimensional form, the following parameters are defined.

$$\text{Ra} = \frac{g\beta L_{\text{ref}}^3 \Delta T}{\eta \alpha}, \quad \text{Pr} = \frac{\eta}{\alpha}; \quad \text{where } \eta = \frac{\mu}{\rho}, \quad \alpha = \frac{k}{\rho C_p} \quad (5)$$

$$X = \frac{x}{L_{\text{ref}}}, \quad Y = \frac{y}{L_{\text{ref}}}, \quad U = \frac{u L_{\text{ref}}}{\alpha}, \quad V = \frac{v L_{\text{ref}}}{\alpha}, \quad \tau = \frac{\alpha t}{L_{\text{ref}}^2} \quad (6)$$

$$P = \frac{\rho L_{\text{ref}}^2}{\rho \alpha^2}, \quad \theta = \frac{T - T_0}{\Delta T}, \quad \Delta T = T_h - T_c$$

The definitions of the parameters used are available at the nomenclature section. The average Nusselt number is defined as follows:

$$\text{Nu} = - \int_0^1 Y \left. \frac{\partial \theta_s(Y)}{\partial X} \right|_{X=0,1} dY \quad (7)$$

Where,  $\theta_s(Y)$  is the dimensionless local temperature at the heated surface.

#### 3.3 Boundary Condition

For the Navier-stokes equation, the boundary conditions are no slip for all walls and for the energy equation; the side walls been maintained at differentially heated condition and the top and the bottom walls have been considered as adiabatic. The left and the right walls have been maintained as hot and cold wall, respectively. The boundary conditions and the flow domains are illustrated in Fig. 1. Mathematically those can be written as non-dimensional form.

$$\text{Bottom surface} \quad U = 0; \quad V = 0; \quad \frac{\partial \theta}{\partial Y} = 0 \quad (8)(a)$$

$$\text{Top surface} \quad U = 0; \quad V = 0; \quad \frac{\partial \theta}{\partial Y} = 0 \quad (8)(b)$$

$$\text{Left surface} \quad U = 0; \quad V = 0; \quad \theta = 1 \quad (8)(c)$$

$$\text{Right surface} \quad U = 0; \quad V = 0; \quad \theta = 0 \quad (8)(d)$$

### 4. Numerical Modeling

#### 4.1 Computational Procedure

The set of partial differential equations (1)-(4) with boundary conditions (8) are non-linear and coupled hence, difficult to solve them analytically. So, the momentum and energy balance equations have been solved by using the Galerkin weighted residual finite element technique. The continuity equation has been used as a constraint due to mass conservation. The basic unknowns for the above differential equations are the velocity components (U, V), the temperature  $\theta$  and the pressure P. The computational domain has been discretized with Non-uniform grids of triangular elements with denser grids clustering in regions near the heat source and the enclosed walls. The six noded triangular elements are used in this paper for the development of the finite element equations. The finite element (FE) model is implemented with two types

of triangular Lagrange element: an element with linear velocity and pressure interpolations for the continuity and momentum equations and an element with a quadratic basis velocity and temperature interpolations for the energy equation. A stationary non-linear solver is used together with Direct (UMFPACK) linear system solver. These non-linear equations are solved iteratively using Broyden's method with a LU-decomposition pre-conditioner, always starting from a solution for a nearby Rayleigh number. The convergence of solutions is assumed when the relative error for each variable between consecutive iterations is recorded below the convergence criterion  $\delta$  such that

$$\left| \frac{\Gamma^{n+1} - \Gamma^n}{\Gamma^{n+1}} \right| < \delta \quad (9)$$

Where  $n$  is the Newton's iteration index and  $\Gamma = U, V, P$  and  $\theta$ . The convergence criterion is set to be  $10^{-6}$ .

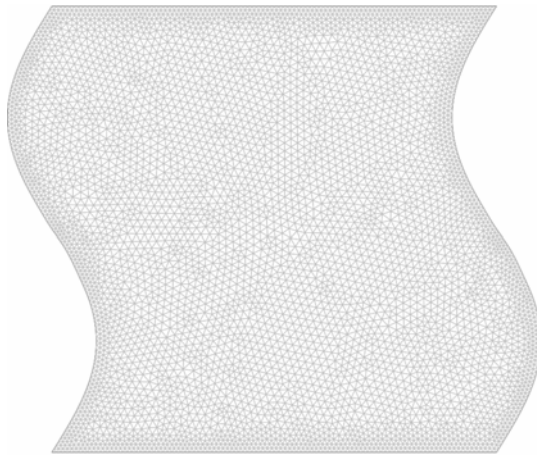


Fig 2. A sample grid showing the major features of the non-uniform triangular meshes adopted in this study

#### 4.2 Grid Refinement Check

To test and assess grid independence of the present solution scheme, many numerical runs are performed for higher Rayleigh number as shown in Fig 2. These experiments reveal that a non-uniform spaced grid of 7873 elements is adequate to describe correctly the flow and heat transfer process inside the enclosure.

Table 1: Comparison of the Results for the Validation of the Code at  $Pr = 0.71$  and  $E/L_{ref} = 0.5$

Rayleigh Number	Average Nusselt number		Error (%)
	Present	Morsi and Das[7]	
$6 \times 10^3$	2.258	2.247	0.49
$8 \times 10^4$	2.456	2.447	0.37
$1 \times 10^4$	2.617	2.601	0.62
$2 \times 10^4$	3.171	3.151	0.63
$4 \times 10^4$	3.840	3.81	0.79

#### 4.2 Code Validation

In order to validate the numerical model, the results are compared with those reported by Morsi and Das [7], considering isothermal heating condition as shown in Table 1. The agreement is found to be excellent which validates the present computations and lend us confidence for the use of the present code.

#### 5. RESULT AND DISCUSSION

For this transient analysis, the working fluid is air with Prandtl number,  $Pr$  being 0.72. The range of Rayleigh number,  $105 \leq Ra \leq 108$ , corrugation amplitude,  $0.1 \leq CA \leq 0.5$  and corrugation frequency,  $1 \leq CF \leq 5$ . To observe the effect of Rayleigh number,  $Ra$ ; corrugation amplitude,  $CA$  and frequency,  $CF$  are kept constant, for understanding the effect of  $CF$ ; the  $Ra$  and  $CF$  are kept constant and to observe the effect of  $CF$ ;  $Ra$  and  $CA$  are kept constant. The numerical results show that the aforementioned parameters have significant effects on the fluid flow and heat transfer for the case considered.

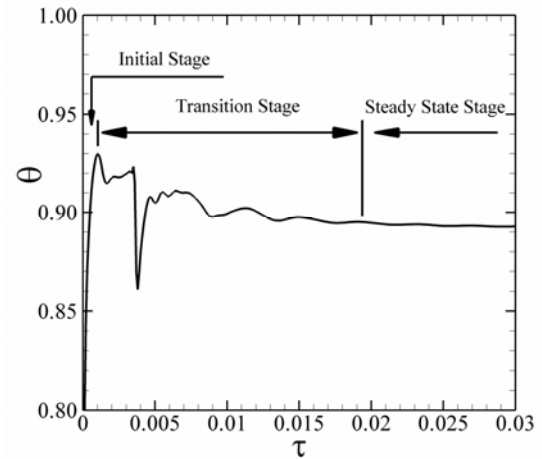


Fig 3. Dimensionless temperature,  $\theta$  versus dimensionless time,  $\tau$  plot at point (0.01, 0.5) for  $Ra = 10^7$ ,  $CA = 0.1$  and  $CF = 1$

#### 5.1 Effect of Rayleigh Number

Fig 3 shows the consequent transient behavior at a point very close to the hotter left wall. It clearly demonstrates the three stages, (a) the initial rising stage (up to  $\tau = 0.001$ , approximately) (b) intermediate transitional stage (up to  $\tau = 0.02$ , approximately) (c) steady state stage for the consequent behavior oh sudden heating. In the initial stage the development of the boundary layer is dominated by pure conduction, the transitional stage is dominated by formation of several overshoots and undershoots. Finally, the steady stage is dominated by convection. This three stages of flow development can be easily identified in figure 3.

In fig 4, dimensionless temperature,  $\theta$  has been plotted against dimensionless time,  $\tau$  for different Rayleigh number,  $Ra$  at point very close the hotter left wall. The coordinate of the point is 0.001, 0.5. It shows,

the temperature at that point decreases as Rayleigh number increases. This is because for higher Ra value the thermal layer thickness is lower, as a result the maximum temperature for the higher Ra concentrated near the left wall. More oscillation can be seen for higher Rayleigh number which confirms the presence of travelling waves of the boundary layer for higher Ra values. Moreover, it takes more time for the boundary layer to become steady state for lower values compare to the higher value of Ra.

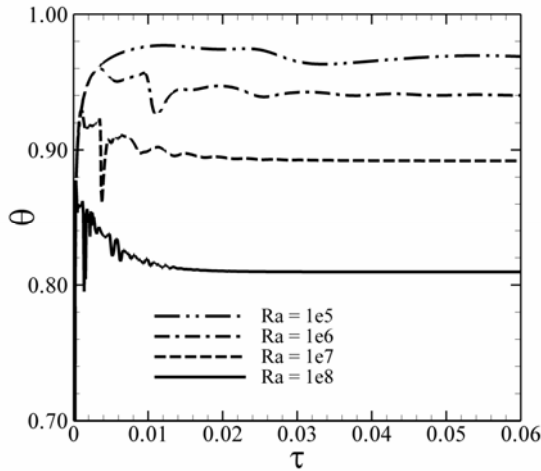


Fig 4. Dimensionless temperature,  $\theta$  versus dimensionless time,  $\tau$  plot for different values of Ra at point (0.01, 0.5), while CA = 0.1 and CF = 1

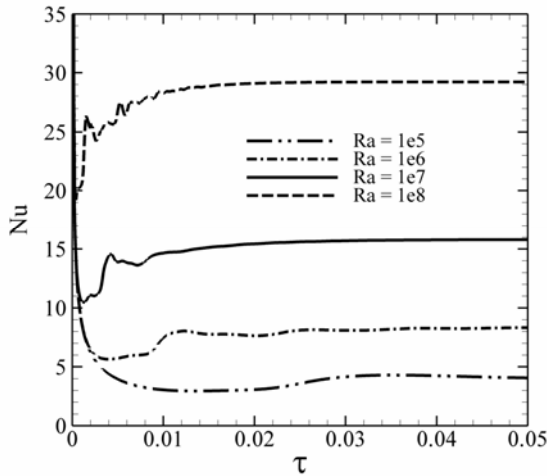


Fig 5. Average Nusselt number, Nu along the hot left wall versus dimensionless time,  $\tau$  for different Ra, while CA = 0.1 and CF = 1.

Fig 5 represents the average Nusselt number along the hot left wall against dimensionless time,  $\tau$  for different Rayleigh number, Ra. Fig 5 demonstrates the three stages of flow development to the initial rising stage, the intermediate transitional stage and the steady state stage i.e. the Nusselt number sharply decreases which is the

initial stage of the flow development. Then it enters the second stage (transitional stage) where it shows few oscillations and at the end the heat transfer becomes constant at steady stage. It also shows that average Nusselt numbers increase with increasing Rayleigh number as a results of strong convection effect.

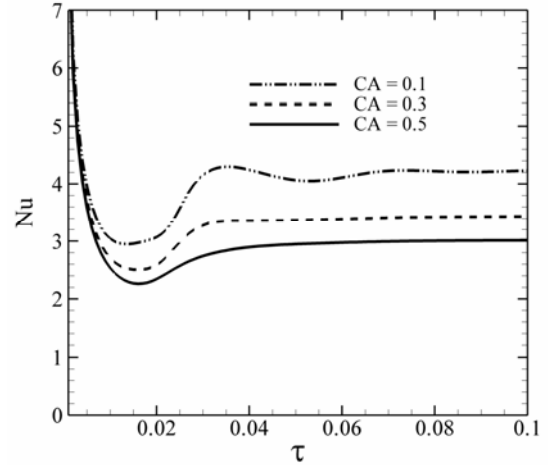


Fig 6. Average Nusselt number, Nu along the hot wall versus dimensionless time,  $\tau$  for different CA, while Ra =  $10^5$ , CF = 1

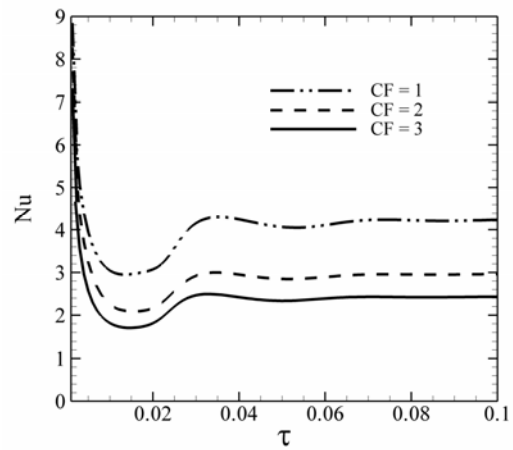


Fig 7. Average Nusselt number, Nu along the hot wall versus dimensionless time,  $\tau$  for different CF, while Ra =  $10^5$ , CA = 0.1

## 5.2 Effect of Corrugation Amplitude and Frequency

Fig 6 and 7 show the variation of average Nusselt number with dimensionless time for different corrugation amplitude, CA and corrugation frequency, CF respectively. The nature of these two curves is similar. Both show an initial, sharp decrease in average Nusselt number followed by an oscillatory stage. After the oscillatory period the average Nusselt number reaches to a steady value. For both of corrugation amplitude and

frequency increases, the time required to attain steady value decreases. Both fig 6 and 7 shows decrease in average Nusselt Number for increasing corrugation amplitude and frequency.

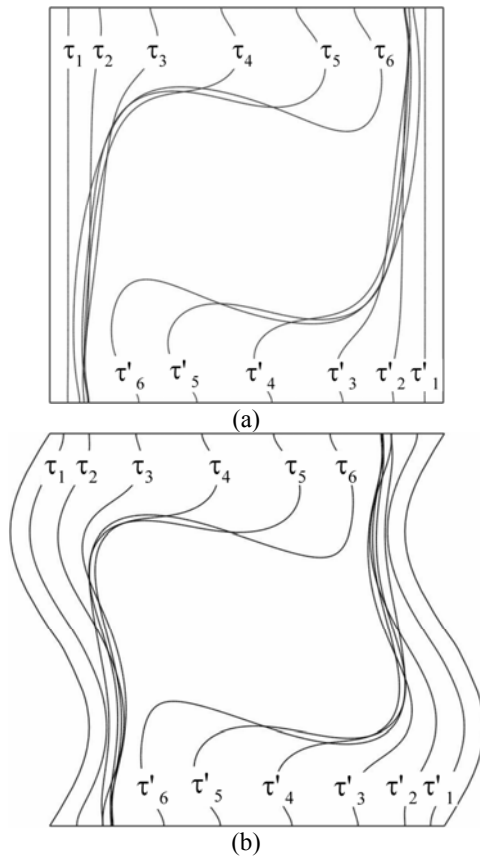


Fig 8. Development and transition of thermal layer along hotter left wall and colder right wall for isotherm magnitude of 0.35 and 0.65 at different dimensionless time,  $\tau$  (a) perfect square, (b) modified square with corrugated sidewalls  $\tau_1 = 0.001$ ,  $\tau_2 = 0.005$ ,  $\tau_3 = 0.010$ ,  $\tau_4 = 0.015$ ,  $\tau_5 = 0.020$ ,  $\tau_6 = 0.025$

## 5.2 Development of Thermal Boundary Layer

Fig 8 shows the development and transition of a certain thermal layer for different dimensionless time,  $\tau$ . Initially, thermal layers from differentially heated walls begin to originate. With time these layers start to move from the boundary region toward the core region of the enclosure. As the cold and hot thermal layers gradually move into the mid section of the enclosure, the hot thermal layers shows an intrusion at the top section of the enclosure along the top adiabatic wall while the cold thermal layers demonstrate the same phenomena at the bottom section along the bottom adiabatic wall. The top and bottom intrusive layers also tend to move toward the central or the core region while moving along the top and bottom flat adiabatic walls. At some point, thermal layers form differentially heated walls collide at the core region of the enclosure. This is a very unstable period during

this period of time; the thermal layers oscillate back-and-forth for a certain period of time. During this period, these oscillations gradually diminish as the colliding thermal layers tend to settle down. After this oscillating period, those colliding thermal layers attain a stable orientation and the final stage i.e the steady state stage is attained.

The development and transition of thermal layer for a perfect square has also been shown in fig 8 (a). This has been done to demonstrate a comparison with the development and transition of thermal layer of the considered computational domain.

## 6. CONCLUSION

A numerical study has been carried out on unsteady natural convection within a modified square enclosure with sinusoidal side walls. The objective of this study was to observe the effect of sudden heating and consequent transient behavior over thermal boundary layer development. The important outcomes of the present investigation are as follows:

(1) The numerical results reveal that the development of natural convection flows in the corrugated cavity undergoes three main stages: an initial stage, a transitional stage and a steady stage.

(2) For a convective fluid, for the model considered, having all other parameters kept constant, for the range of Rayleigh number,  $Ra$  from  $10^5$  to  $10^8$ , the time required to attain steady state reduces as the value of Rayleigh number increases.

(3) Corrugation parameters have significant impact on the thermal behavior and on the development of thermal boundary layer.

(4) Increase in both corrugation amplitude and corrugation frequency reduces the heat transfer rate, indicated by the reduction of average Nusselt number.

## 7. REFERENCES

1. Xu F., Patterson J.C., Lei C., 2005, "Shadowgraph observations of the transition of the thermal boundary layer in a side-heated cavity", *Experiments in Fluids* 38: 770–779.
2. Xu F., Patterson J.C., Lei C., 2008, "On the double-layer structure of the boundary layer adjacent to a sidewall of a differentially heated cavity", *International Journal of Heat and Mass Transfer* 51, pp. 3803–3815.
3. Xu F., Patterson J.C., Lei C., 2010, " $Pr > 1$  intrusion flow induced by a vertical heated wall", *Physical Review E* 82: 026318-1 - 026318-10
4. Siegel R., 1958, "Transient free convection from a vertical flat plate", *Journal of Heat Transfer* 80: 347–360
5. Brown S.N., Riley N., 1973, "Flow past a suddenly heated vertical plate", *Journal of Fluid Mechanics* 59: 225–237
6. Patterson J.C., Imberger J., 1980, "Unsteady natural convection in a rectangular cavity", *Journal of Fluid Mechanics* 100: 65–86.

7. Morsi, Y. S. and Das, S., 2003, "Numerical Investigation of Natural Convection inside Complex Enclosures," Heat Transfer Engineering, Vol. 24(2), pp. 30-41.

## 8. NOMENCLATURE

Symbol	Meaning	Unit
$C_p$	Specific heat capacity	J/Kg.K
CA	Dimensionless amplitude of the corrugation	
CF	amplitude of the corrugation	
g	gravitational acceleration	m/s <sup>2</sup>
h	convective heat transfer coefficient	W/m <sup>2</sup> K
H	height of the enclosure	m
L	width of the enclosure	m
$L_{ref}$	reference length	m
Nu	Nusselt number, Eq.(5)	
P	pressure	N/m <sup>2</sup>
p	dimensionless pressure,	
Pr	Prandtl number, $[v/\alpha]$	
q	heat flux	W/m <sup>2</sup>
Ra	Rayleigh Number	
T	temperature	K
$T_o$	initial temperature	K
u	velocity component in x-direction	m/s
U	dimensionless velocity component in X-direction	
v	velocity component in y-direction	m/s
V	dimensionless velocity component in Y-direction	
x, y	Cartesian co-ordinates	m
X, Y	dimensionless Cartesian co-ordinates	
Greek Symbol		
$\Gamma$	dummy variable	

$k$	thermal conductivity of fluid	W/mk
$\alpha$	thermal diffusivity	m <sup>2</sup> /s
$\beta$	coefficient of volumetric expansion	1/K
$\theta$	dimensionless temperature	
$\theta_s$	local dimensionless surface temperature	
$\lambda$	wave length of the sinusoidal corrugation	m
$\nu$	kinematic viscosity	m <sup>2</sup> /s
$\rho$	fluid density	kg/m <sup>3</sup>

Subscript		
av	average	
c	cold wall	
h	hot wall	
o	initial	
p	constant pressure	
ref	reference	
s	surface	

## 9. MAILING ADDRESS

### Muhammad Noman Hasan

Department of Mechanical Engineering,  
BUET, Dhaka-1000, Bangladesh.  
Email: [noman.becker@gmail.com](mailto:noman.becker@gmail.com),

### Suvash C. Saha

School of Engineering Systems,  
Queensland University of Technology,  
Brisbane QLD 4001, Australia  
Email: [s\\_c\\_saha@yahoo.com](mailto:s_c_saha@yahoo.com)

### Y. T. Gu

Email: [yuantong.gu@qut.edu.au](mailto:yuantong.gu@qut.edu.au)